



Spatiotemporal Variability, Trend, and Change-Point of Precipitation Extremes and Their Contribution to the Total Precipitation in Iran

AZAR ZARRIN¹  and ABBASALI DADASHI-ROUDBARI¹

Abstract—The present study analyzes the observed extreme precipitation based on the daily precipitation records of 49 ground stations across Iran from 1980 to 2019. The present study aims to investigate the frequency, intensity, and trend of precipitation extremes in different climate zones. We computed the new extreme precipitation indices (EPI) recommended by the Expert Team on Sector-Specific Climate Indices (ET-SCI) and used two nonparametric tests, the modified Mann–Kendall (MM–K) test and Sen slope estimator (SSE), to identify the trend magnitude. Also, we applied the Buishand test for detecting the potential change-point of EPIs in Iran. The results showed that the consecutive wet days (CWD) are decreasing at 73.47% of the stations in Iran. The annual sum of precipitation in wet days (PRCPTOT) index in 87.76% of Iran showed a decreasing trend, indicating severe drought conditions in Iran. The simple daily intensity index (SDII) in 71.42% (30.23% at the level of 0.05 significance) has an increasing trend. The heavy precipitation index (R10mm) showed a decreasing trend in all zones. The most frequent change-point of extreme precipitation occurred in 1997 and 1998 on Iran’s west, southeast, and southern coasts. Increasing the intensity of precipitation along with decreasing in precipitation frequency has caused the increased contribution of extreme precipitation to the total annual precipitation in Iran.

Keywords: Climate extremes, trend analysis, ET-SCI Indices, change-point detection (CPD), Iran.

1. Introduction

Extreme precipitation is the subject of extensive research based on many indices and methods (Alexander et al., 2019; Donat et al., 2013, 2017). Any changes in extreme precipitation and its contribution to the annual precipitation profoundly affect the natural environment and human society. It can affect water resources (Cardoso Pereira et al., 2020),

the environment (Prein et al., 2017), agriculture (Carpenter et al., 2018), socioeconomic systems (Zhang et al., 2018), and health (IPCC, 2012).

Extreme precipitation-related natural disasters have increased in recent years. About 90% of natural disasters are caused by climate hazards such as floods, droughts, and heat stresses (UNISDR, 2015). In general, spatial extents of precipitation are heterogeneous, which favors many changes in different climate regimes. Therefore, it is essential to study the characteristics of the trend, such as the intensity and change-point of precipitation and its contribution to the total annual precipitation in different regions of the world (Rahman & Islam, 2019; Trenberth et al., 2003).

Based on the latest reports of the Intergovernmental Panel on Climate Change (IPCC) in the Fifth Assessment Report (IPCC, 2013) and a special report on the impacts of global warming of 1.5 °C (Masson-Delmotte et al., 2018), global warming has increased the frequency, intensity, and duration of extreme precipitation events. Extreme precipitation has intensified in different regions, and RX1day has risen at about two thirds of the world’s stations (Donat et al., 2013, 2019; Westra et al., 2013). Extreme climate events and their variations are crucial to human and natural society due to their potentially severe effects, as stated in the *Special Report on Managing the Risks of Extreme Events and Disasters to Advance Climate Change Adaptation* (SREX) (IPCC, 2012).

The Middle East region is a climate change hotspot in which precipitation events are expected to increase and intensify for all seasons (Tabari & Willems, 2018). Iran is one of the driest regions in the Middle East, with an average annual precipitation of

¹ Department of Geography, Ferdowsi University of Mashhad, Room 32, Azadi Square, Mashhad, Iran. E-mail: zarrin@um.ac.ir

about 250 mm (Javanmard et al., 2010), and has notable climate diversity in terms of spatiotemporal precipitation regimes. However, a significant amount of total annual precipitation falls during the cold period of the year. Geographically, the southern coast of the Caspian Sea and the mountainous regions of Iran receive the most considerable amount of precipitation (Alijani et al., 2008). In addition, the contribution of extreme precipitation to total precipitation in Iran is substantial.

The spatiotemporal distribution and precipitation trend in Iran have been studied by numerous researchers in recent years (Alijani et al., 2008; Ghalhari et al., 2016; Khalili et al., 2016; Najafi & Moazami, 2016; Salehi et al., 2020; Some'e et al., 2012; Zarrin & Dadashi-Roudbari, 2021). These studies have shown a decreasing precipitation trend in most parts of Iran. However, according to climate projections, extreme precipitation and the frequency of consecutive dry days are likely to increase in the future (Hay et al., 2016). Therefore, examining the extreme precipitation variabilities provides essential results for interpreting possible future trends.

Climate extremes, especially extreme precipitation, are the subject of particular research. This includes global studies (Donat et al., 2013, 2017 and 2019; Alexander et al., 2019), continental Asia (Kirschbaum et al., 2020), Africa (Shongwe et al., 2011), North America (Kunkel, 2003), South America (Palharini et al., 2020), and Australia (Wasko et al., 2018). In addition, this topic receives special attention on the regional scale (Dravitzki & McGregor, 2011; Guo et al., 2018; Heureux et al., 2022; Li et al., 2015; Talchabhadel et al., 2018).

Many researchers have analyzed the extreme precipitation in the region of the Middle East, including Iran (de Vries et al., 2013; Tabari & Willems, 2018; Zhang et al., 2005). Overall, these studies may group into two categories: (1) across Iran (Alavinia & Zarei, 2021; Darand et al., 2017; Mahbod & Rafiee, 2021; Najafi & Moazami, 2016; Rahimi & Fatemi, 2019; Rahimzadeh et al., 2009; Soltani et al., 2016; Tabari et al., 2014) and (2) some specific regions of Iran (Kiany et al., 2020). Some studies have examined the synoptic patterns associated with extreme precipitation events (Rousta et al., 2020; Shaffie et al., 2019).

Despite many works that reviewed extreme precipitation over Iran, two aspects of them have received less attention. Most of the studies conducted for precipitation extremes only used 95th and 99th percentiles of precipitation in Iran (Fathian et al., 2020; Ghiami-Shamami et al., 2019; Rahimi & Fatemi, 2019; Rahimzadeh et al., 2009; Soltani et al., 2016). We have used the new Expert Team on Sector-specific Climate Indices (ET-SCI) recommended by the World Meteorological Organization (WMO) along with the Expert Team on Climate Change Indicators Detection and Indices (ET-CCDI). The most recent research that investigated extreme precipitation in Iran (Alavinia & Zarei, 2021; Mahbod & Rafiee, 2021) has examined only percentile indices, and they did not focus on ETCCDI. Also, no study has investigated the contribution of extreme precipitation to total precipitation in Iran.

Compared to similar studies conducted on extreme precipitation in Iran, this research investigates the new indices recommended by ET-SCI, detects the extreme precipitation time series change-point, determines the contribution of extreme precipitation to total annual precipitation, and finally applies the modified Mann–Kendall for trend detection. Extreme precipitation and its contribution to total annual precipitation in recent decades in Iran has shown complex variability. Therefore, this study aims to analyze extreme precipitation to distinguish the contribution of the leading precipitation indices to the total annual precipitation in Iran.

This paper provides a comprehensive extreme precipitation analysis in Iran, which is organized into five main sections. Section 1 presents an investigation of Iran's extreme precipitation based on the recommended indices of ET-SCI and ETCCDI. Section 2 presents computation of the trend and slope estimator of extreme precipitation studied based on the modified Mann–Kendall and Sen methods. Section 3 presents attempts to detect the change-point of Iran extreme precipitation. Section 4 presents an investigation of the contribution of extreme precipitation to total precipitation, and Sect. 5 presents calculation of cross-correlation extreme precipitation indices (EPIs) in Iran. Comparing the findings of this paper with the results of previous studies (such as Alavinia & Zarei, 2021; Mahbod & Rafiee, 2021;

Rahimi & Fatemi, 2019) will improve our knowledge of extreme precipitation and provide a better interpretation of its changes.

2. Material and Methods

2.1. Description of the Study Area

Iran, located between 25°30'N to 39°47'N and 44°5'E to 63°18'E, with a predominantly hot and dry climate, has a variety of climates ranging from Cfa to Bwh based on Köppen–Geiger climate classification. Accordingly, climatic diversity is evident in the spatiotemporal distribution of precipitation. In this research, we aim to investigate extreme precipitation in different climate zones of Iran. For this purpose, we used the Köppen–Geiger climate classification method. Of the 31 Köppen–Geiger climate classes, 13 are reorganized in Iran (Fig. 1). The predominant climates of Iran are desert (BW, in the east and southeast of Iran) and semi-desert (BS, in the northeast of Iran), and the temperate climate is limited to small parts of the Zagros and the southern coast of the Caspian Sea (Zarrin & Dadashi-Roudbari, 2021). We selected 49 synoptic stations with long-term records (1980–2019) in seven climate zones including Bsh (three stations), BsK (12 stations), BWh (15 stations), BWk (eight stations), Cfa (one station), Csa (five stations), and Dsa (five stations).

2.2. Selection of Synoptic Stations

Extreme precipitation is statistically infrequent, and the study of the characteristics of these precipitation events and the determination of their trend is closely related to the accuracy of daily data and missing values. Daily precipitation data used in this study were obtained from the Iran Meteorological Organization (IRIMO). There are 414 synoptic stations in Iran, of which only 50 stations have 40-year long-term records (1980–2019). Therefore, selected stations in this study were examined for completeness, quality, and homogeneity.

2.3. Completeness

Stations containing missing values for more than 10% (Zolina et al., 2005) of their total daily time series (1980–1920) were removed from the data set. The lack of more than 10% in the selected time series is not acceptable due to the sensitivity of the linear trend of daily precipitation time series. Accordingly, Hamedan (Nozheh), Dezful (Airport), Omidiyeh (Air Base), Omidiyeh (Aghajari), Tabas, and Bushehr (Coastal) stations were removed from the data set. Finally, 49 stations were selected for a statistical period of 40 years (Fig. 1).

2.4. Quality Control

To identify suspicious data from a 40-year time series, two conditions were used for this purpose (Ghiami-Shamami et al., 2019; Mahbod and Rafiee, 2021; Soltani et al., 2016): (1) data with more than three standard deviations from daily values; and (2) duplicate data of more than 10 days with nonzero values. Applying the above two conditions for the time series of 49 selected stations in Iran does not show this, so the quality of the data is approved.

2.5. Homogeneity

As mentioned, after applying the quality control criteria and completeness of the data from 55 stations, six stations were left out. Based on this, 49 synoptic stations with complete and homogeneous data were selected (Fig. 1). As shown in Fig. 1, the selected stations with appropriate spatial distribution are scattered throughout Iran, and the homogeneity of these data is confirmed at $\alpha = 0.05$.

2.6. ETCCDI and ET-SCI Indices of Precipitation Extremes

There are several ways to study climate extremes. Some studies look at extraordinary or record-breaking events over a certain time frame (Beniston, 2015), and many studies look at absolute thresholds or percentiles. Leander et al. (2014), Schär et al. (2016), and many other studies use extreme value theory (EVT) to compute return periods (Kharin et al., 2013;

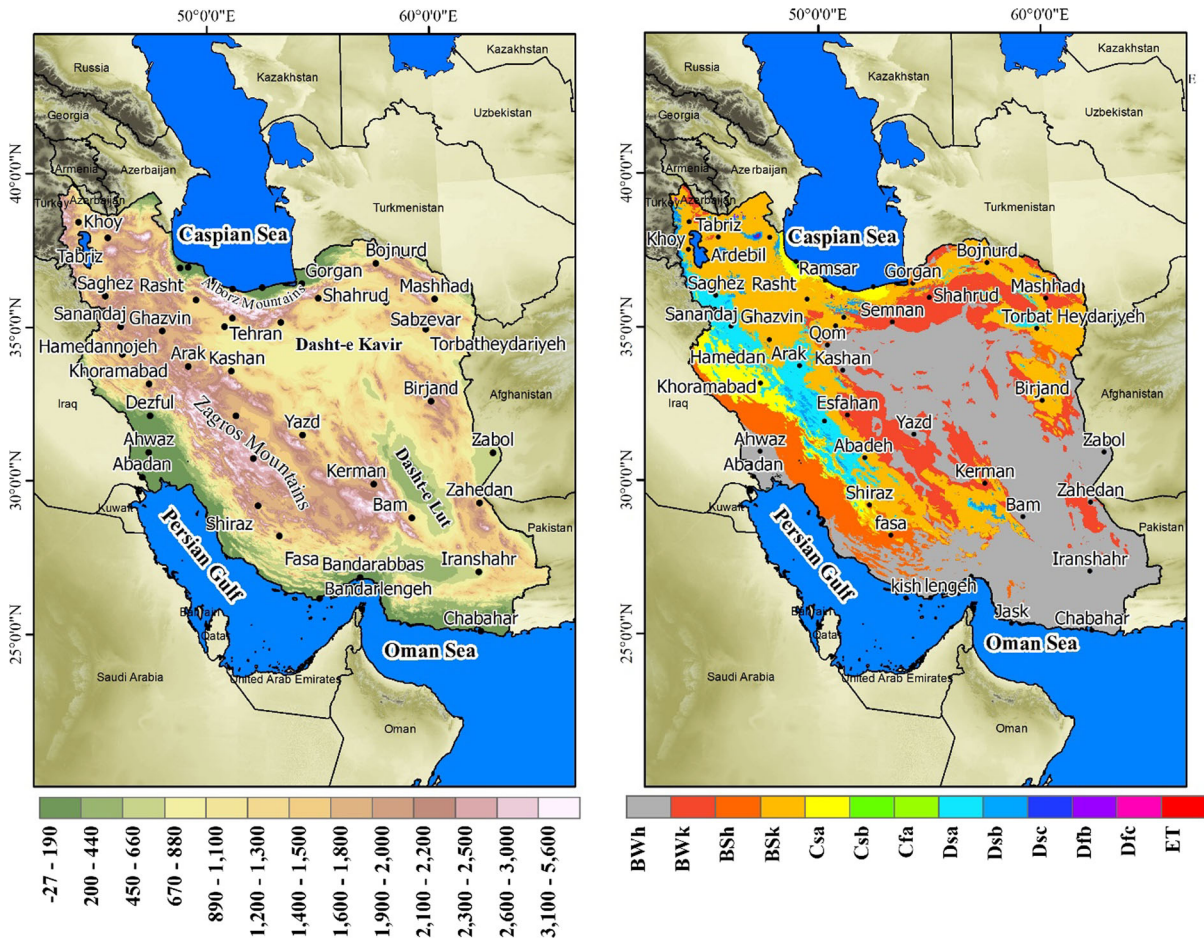


Figure 1

a) Location of ground stations used in this study. Shaded color represents topography. b) Köppen–Geiger climate classification [0.0083° resolution (approximately 1 km at the equator)] (Beck et al., 2018)

Tebaldi & Wehner, 2018). To facilitate the analysis of temperature and precipitation extremes, the new ET-SCI recommended by the WMO along with the ET-CCDI has defined a set of climate change indices focusing on extreme events. These indices generally describe extreme events, with a time step of 1 year or less (Zhang et al., 2011) widely used in IPCC reports (Hoegh-Guldberg et al., 2018; IPCC, 2012; Stocker et al., 2013). In this study, we used 12 extreme precipitation indices in three groups of duration, frequency, and intensity from ETCCDI and ET-SCI (Table 1).

3. Statistical Methods

3.1. Calculation of Extreme Precipitation Trend [Modified Mann–Kendall [MM–K]]

The modified Mann–Kendall (MM–K) test was used to analyze the trend analysis in the long-term data series. In this test, H_0 indicates the absence of a trend, and H_1 indicates the trend in the time series of data (Mann, 1945; Kendall, 1948). The Z score in the MM–K test follows the standard normal distribution with an average of zero and a variance of 1 and is used to measure the trend (Liu et al., 2014). It should be noted that the rejection of H_0 in this test does not mean that there is no trend in the time series. Instead,

Table 1
 List of selected extreme precipitation indices (EPIs) (adapted from ET-SCI) (Chapagain et al., 2021)

Category	Indices ID	Long name	Calculation	Definition	Units
Duration indices	CDD	Consecutive dry days	Maximum annual number of consecutive dry days (when PR ≤ 1.0 mm)	The longest dry spell	Days
	CWD	Consecutive wet days	Maximum annual number of consecutive wet days (when PR ≥ 1.0 mm)	The longest wet spell	Days
Frequency indices	R10mm	Number of heavy precipitation days	Number of days when precipitation ≥ 10 mm	Days when precipitation is at least 10 mm	Days
	R20mm	Number of very heavy precipitation days	Number of days when precipitation ≥ 20 mm	Days when precipitation is at least 20 mm	Days
	R30mm	Number of extremely heavy precipitation days	Number of days when precipitation ≥ 30 mm	Days when precipitation is at least 30 mm	Days
Intensity indices	SDII	Daily PR intensity	Annual total precipitation divided by the number of wet days (when total PR ≥ 1.0 mm)	Average daily wet-day precipitation intensity	mm/day
	RX1day	Greatest 1-day precipitation	Maximum 1-day precipitation total	Maximum amount of precipitation that falls in one day	mm
	RX3day	Greatest 3-day precipitation	Maximum 3-day precipitation total	Maximum amount of precipitation that falls in three days	mm
	RX5day	Greatest 5-day precipitation	Maximum 5-day precipitation total	Maximum amount of precipitation that falls in five consecutive days	mm
	PRCPTOT	Total precipitation in wet days	Sum of daily precipitation ≥ 1.0 mm	Total wet-day precipitation	mm
	R95pTOT	Contribution from extremely wet days	Annual sum of daily precipitation above the 95th percentile	Fraction of total wet-day precipitation that comes from very wet days	mm
	R99pTOT	Contribution from extremely wet days	Annual sum of daily precipitation above the 99th percentile	Fraction of total wet-day precipitation that comes from extremely wet days	mm

it shows that the available evidence is insufficient to conclude that there is no trend in the time series (Dadashi -Roudbari & Ahmadi, 2020; Maghrabi & Alotaibi, 2018).

The MK test statistic (S) of a data series, y having n data points, is estimated as (Mann, 1945)

$$S = \sum_{i=1}^{n-1} \sum_{j=i+1}^n \text{sgn}(x_j - x_i), \tag{1}$$

where

$$\text{sgn}(x_j - x_i) = \begin{cases} 1 & \text{if } (x_j - x_i) > 0 \\ 0 & \text{if } (x_j - x_i) = 0 \\ -1 & \text{if } (x_j - x_i) < 0 \end{cases} \tag{2}$$

The variance of S [$V(S)$] is used to estimate Z statistics to decide trend significance:

$$Z = \begin{cases} \frac{S-1}{\sqrt{V(s)}} & \text{if } s > 0 \\ 0 & \text{if } s = 0 \\ \frac{S+1}{\sqrt{V(s)}} & \text{if } s < 0 \end{cases} \tag{3}$$

The MM-K test can be used only if Z is found to be significant in the Mann-Kendall (MK) test. The MM-K test evaluates whether the MK trend is due to the natural variability of climate or due to a global warming-induced unidirectional trend (Pour et al., 2020). The MM-K test de-trends the time series (Hamed, 2008).

The significance of H is decided by Pour et al. (2020) by the use of first and second moments for $H = 0.5$. For significant H , the variance of S is estimated as

$$V(S)^H = \sum_{i < j} \sum_{k < l} \frac{2}{\pi} \sin^{-1} \left(\frac{\rho|j-i| - \rho|i-l| - \rho|j-k| + \rho|i-k|}{\sqrt{(2-2\rho|i-j|)(2-2\rho|k-l|)}} \right) \quad (4)$$

Here, $V(S)^H$ is the biased estimate of the variance of S which can be eliminated through the use of a correction factor (B):

$$V(S)^H = V(S)^H \times B \quad (5)$$

The significance of the MM-K test is determined by using $V(S)^H$ instead of $V(S)$ in Eq. (4).

3.2. Calculation of the Trend Slope of Precipitation Extremes (Nonparametric SSE Test)

The nonparametric Sen's slope estimator (SSE) method can estimate the actual trend slope in the time series (Yue & Hashino, 2003). This method was first proposed by Theil (1950) and then developed by Sen (1968). We used the SSE method to estimate trends in extreme precipitation. Mathematically, it is represented as Eq. 6:

$$Q = \text{median} \left[\frac{\Delta y}{\Delta t} \right] \quad (6)$$

where Δy is the change of recorded values due to change time, and Δt is between two successive data points in the time series (Pour et al., 2020).

3.2.1 Nonparametric Change-Point Detection (Buishand)

In this study, the change-point of extreme precipitation was investigated using the nonparametric Buishand test (Buishand, 1982). The change-point is when the time series of the data previously has a definite distribution with a mean γ_0 and for subsequent years has a definite distribution with a mean γ_1 . The point estimator is used to detect abrupt changes between two consecutive differences. In the Buishand test, the null hypothesis, H_0 indicates the absence of a change-point in the time series, and H_1 indicates the existence of a change-point in the data series used at an unknown point.

$$S_0 = 0, S_k^* = \sum_{i=0}^k (x_i - \mu), k = 1, 2, \dots, T \quad (7)$$

$$S_k^{**} = \frac{S_k^*}{\sigma} \quad (8)$$

$$Q = 0 \leq \max_k < T |S_k^{**}| \quad (9)$$

where, S refers to statistics of data homogeneity, and if they are close to zero, the data series are homogeneous. x_i = time series values. μ = arithmetic mean of time series values of the desired parameter. σ = standard deviation of time series. T = time; and Q = critical values of the test that can vary from zero to infinity (Dadashi-Roudbari & Ahmadi, 2021). In the present study, the significance of the Buishand result was tested at the 95% confidence level using the Monte Carlo method.

3.3. Spearman's Rank Correlation Coefficient

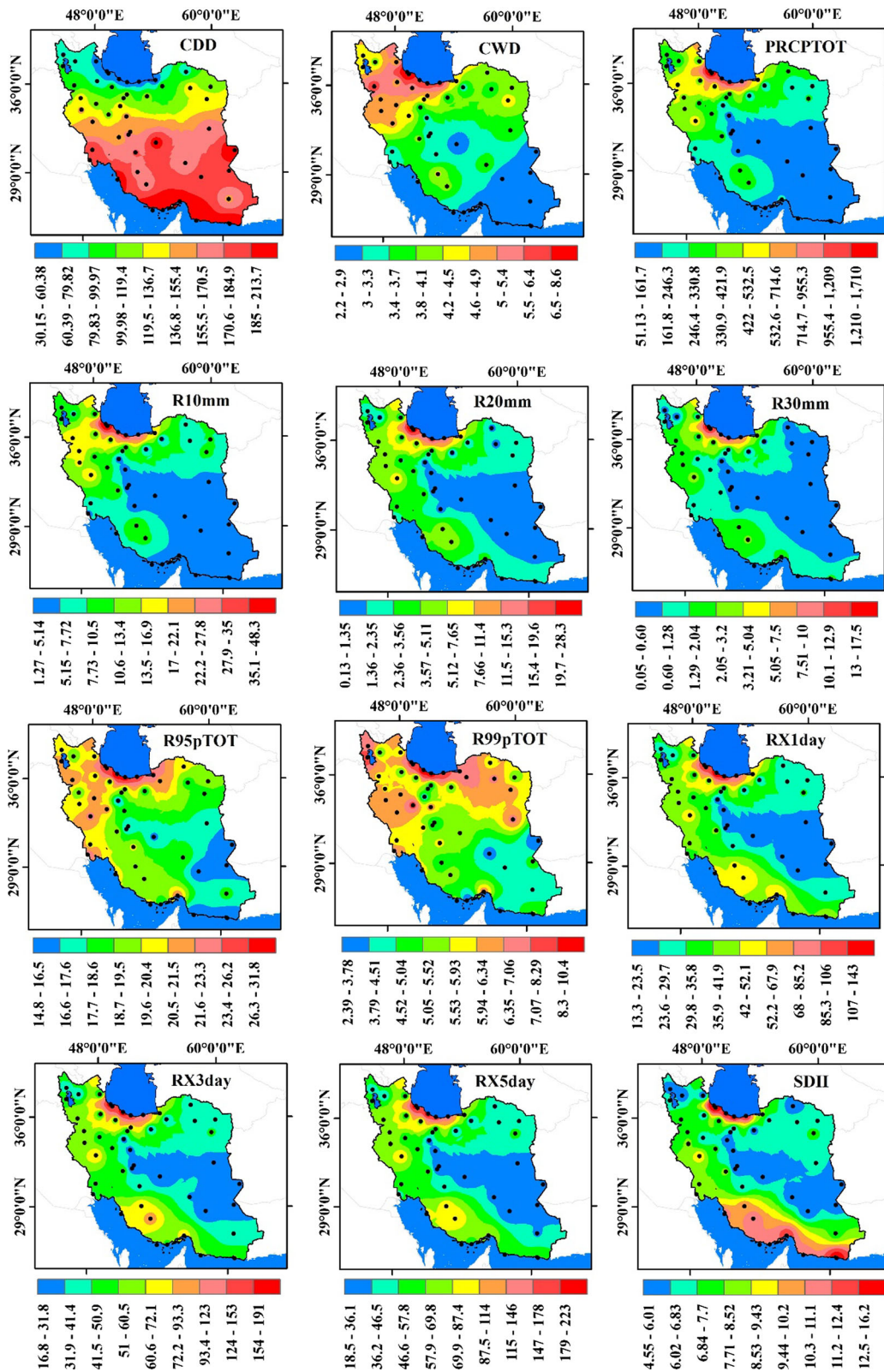
Spearman's rank correlation coefficient was used to examine the relationship between the extreme precipitation indices. Spearman's method is one of the nonlinear methods for analyzing climate variables. Spearman's rank correlation test fluctuates between +1 and -1 (Myers & Sirois, 2004).

4. Results and Discussion

4.1. Percentile-Based Extreme Precipitation

In Iran, the maximum values of R95pTOT and R99pTOT were experienced in the Csb, Csa, and Dsa climate zones (Fig. 2). Geographically, these areas include the Caspian Sea coasts in northern Iran and the Zagros Mountains in western Iran, while the smallest values (less than 20% for the R95pTOT index and less than 5% for the R99pTOT index) for both the R95pTOT and R99pTOT spread in the BWh and BSk climates, especially in central Iran, southeast, and the coasts of the Oman Sea. The values of R95pTOT [14.80 to 31.76%] and R99pTOT [2.39 to 10.43%] indices are decreasing from north to south and west to east of Iran.

The trend of the R95pTOT index at 51.02% of the stations is increasing, but at only 4% of the stations is



◀Figure 2

Spatial distribution of extreme precipitation indices (EPIs) recommended by the Expert Team on Sector-Specific Climate Indices (ET-SCI) in Iran (CDD [unit = day], CWD [unit = day], R10mm [unit = day], R20mm [unit = day], R30mm [unit = day], SDII [unit = mm/day], RX1day [unit = mm], RX3day [unit = mm], RX5day [unit = mm], PRCPTOT [unit = mm], R95pTOT [unit = mm] and R99pTOT [unit = mm])

it statistically significant at the level of 0.05. At 48.98% of the stations, the trend is decreasing, but at only 4.16% of them is it significant at the level of 0.05 (Fig. 3). The R95pTOT index has shown an increasing trend in the mountainous regions of Iran but a decreasing trend in the arid regions of eastern Iran and the interior. So we can conclude that contribution from very wet days in the mountainous regions of Iran has increased in recent years. On the other hand, the R99pTOT has a decreasing trend in all areas of Iran, except for a few stations in the northwest, west, and northeast of Iran, where the contribution from extremely wet days in Iran is decreasing. Rahimzadeh et al. (2009) reported a similar trend for R95 throughout Iran from 1951 to 2003. A comparison of trends with the study of Rahimzadeh et al. (2009) shows that the changes in precipitation in Iran have increased over the last six decades. In Fig. 3, unlike the Csa climate zone, the R95pTOT and R99pTOT trends show a significant increase (the maximum Z score of the MM–K test for R95pTOT is 2.36, which is statistically significant at 0.05).

A critical point about precipitation in the northeast of Iran is the decreasing trend for most indices. These decreasing trends, even for annual precipitation, pose a severe threat to the water resources of northeastern Iran, the Karakum Basin, and the Atrak River.

The coefficient of variation (CV) in the three climate zones of BSh, Cfa, and Csa is positive for both precipitation percentile indices. The CV of R99pTOT in the Cfa climate zone has reached 97.55% in the last four decades. The coefficient of variation of these two indices in the BWh climate zone is entirely decreasing. In the BSK and Dsa climate zones, the CV of R95pTOT is positive, and

R99pTOT is negative, and vice versa in the BWk climate zone.

Of the seven Köppen–Geiger climate classifications for which a representative station exists, the R95pTOT trend is increasing in five climate zones and decreasing in only two climate zones, BWh and BWk. For the R99pTOT index, the average trend is increasing in four zones and decreasing in three zones. Another important factor regarding the extreme precipitation in Iran that has not been addressed so far is the contribution of extreme precipitation indices in the total precipitation of the country.

The contribution of the R95pTOT index in Iran precipitation (Fig. 4) varies between 1.39 and 29.38%. The central and southeastern regions of Iran have the highest contribution of 95th percentile in annual precipitation, so about one third of the total precipitation in these regions includes precipitation with a 95th percentile threshold. In climate zones, the BWh with 16.26% has the highest contribution to the R95pTOT index in annual precipitation, and the Cfa with 1.35% has the lowest contribution in total annual precipitation (Table 2).

Among the 49 stations, only Chabahar and Gorgan detected a change-point for R95pTOT, and Bam, Chabahar, and Khorramabad detected a change-point for R99pTOT (Table 3). The values of these two indices for the abovementioned stations are higher after the change-point than before the change-point which shows a significant upward trend of precipitation among these stations.

4.2. Maximum 1-day, 3-day, and 5-day Precipitation

The average RX1day, RX3day, and RX5day for 49 selected stations for Iran reached 38.80, 54.62, and 60.98 mm, respectively (Fig. 2). These indices showed big changes in the arid climate. As seen in Table 2, the CV of RX1day and RX3day in the BSh climate zone was more than 50%. The variability of these three indices is widespread in Iran; the maximum values for RX1day and RX3day in Iran go with Cfa, Csa, and Dsa climate zones. In the Cfa climate zone, the land–sea interaction, the Dsa climate, and the wind effect of the Zagros Mountains play a vital role in increasing extreme precipitation. The highest

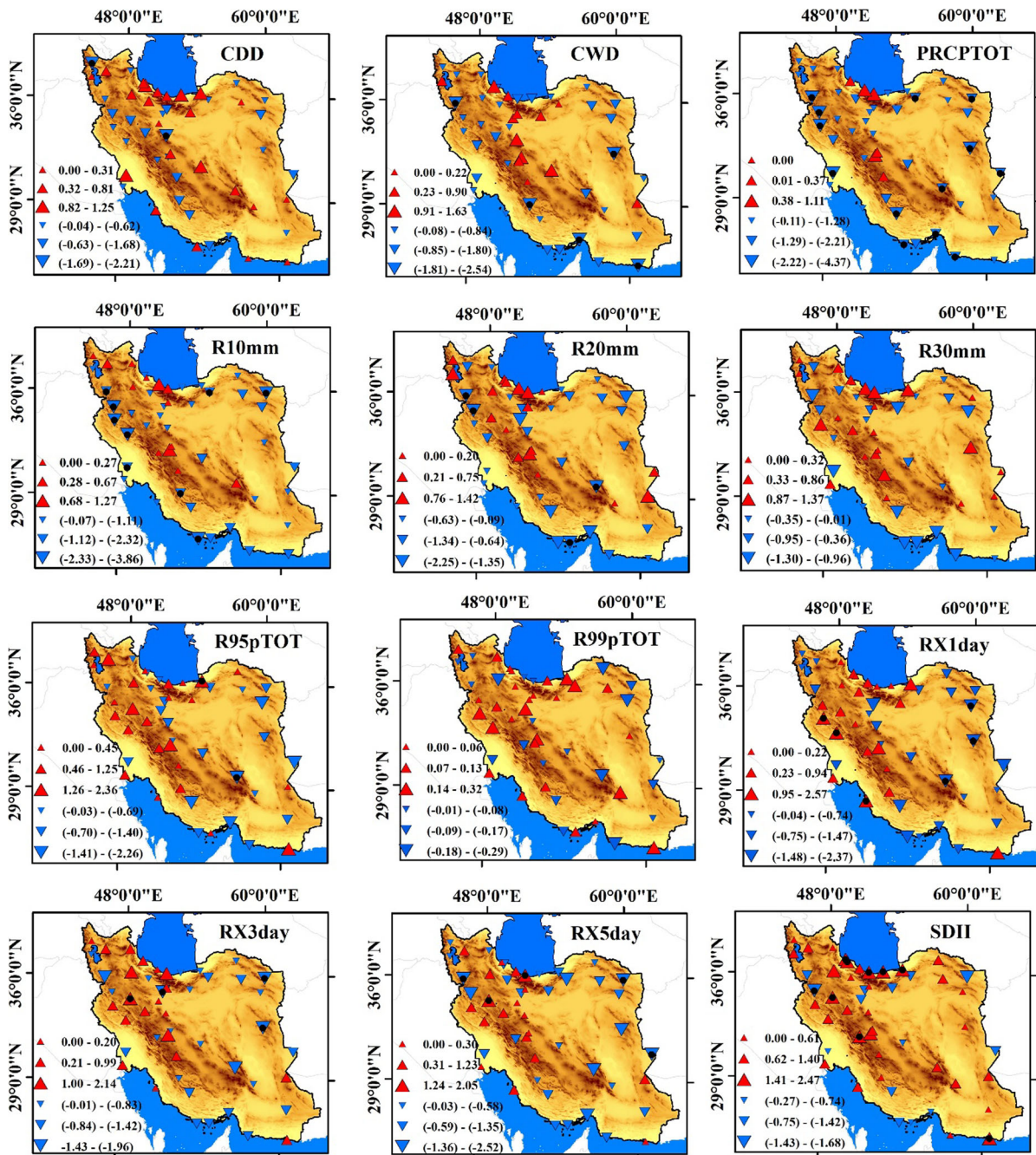
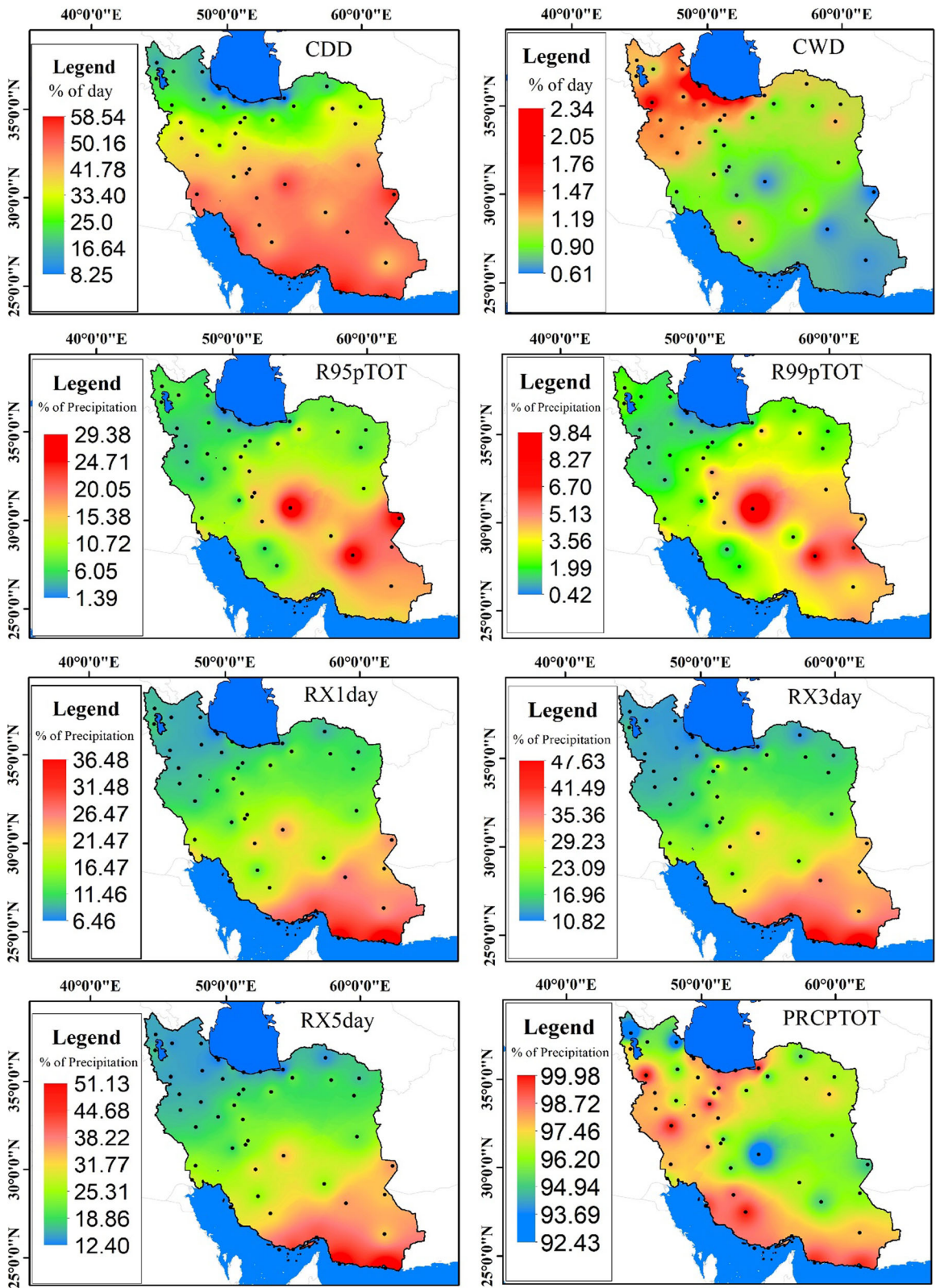


Figure 3

Annual trends of extreme precipitation indices over Iran in 1980–2019 (triangles = increasing trend; upside-down triangles = decreasing trend; inside black dot = significant trend at 95%)

Rx indices are related to the Cfa climate zone located on the southwestern coast of the Caspian Sea. The average RX1day, RX3day, and RX5day indices in the

Cfa climate zone are 113.52, 191.21, and 225.31 mm, respectively (Table 2).



◀Figure 4

The contribution of precipitation extremes to annual total precipitation (ATP) (1980–2019) in Iran (unit = percent)

The Csa climate, which includes the coastal region of the Caspian Sea and the highlands of the Zagros mountains, is the second-most rainy climate zone in Iran. In the Csa climate, the average precipitation for the two indices of RX3day and RX5day is more than 100 mm. The CV of Rx indices in Cfa and Csa climatic zones is positive. In general, in the arid climatic zones of Iran, the contribution of RX1day, RX3day, and RX5day in ATP is higher than in other zones.

In general, all three indices decreased from west to east according to the topography in Iran. The contribution of RX3day in ATP varies from 6.43% in the Cfa climate zone to 35.03% in the BWh climate zone (Fig. 4). In general, in the arid climate zone, the contribution of RX1day, RX3day, and RX5day is higher than in other zones (Fig. 5).

In general, all three indices decreased from west to east in Iran. The contribution of RX3day in ATP varies from a minimum of 6.43% in the Cfa climate zone to a maximum of 35.03% in the BWh climate zone (Fig. 4). In general, in the arid climate zone, the contribution of RX1day, RX3day, and RX5day is higher than in other zones. Applying the MM–K test to selected stations for RX1day, RX3day, and RX5day indices, a significant trend with high oscillation was observed (Fig. 3); therefore, this value of both decreasing and increasing significance is seen less than other precipitation indices.

Examination of station trend changes for RX1day, RX3day, and RX5day indices showed that the Caspian coast and the Zagros mountain chains have the highest increasing trends. A significant increasing trend is evident for the RX1day, RX3day, and RX5day indices, which are 13.63, 5, and 10.52%, respectively. On the other hand, as mentioned before, the trend of precipitation indices in Iran experiences many regional changes, so the extreme indices in inland and eastern regions of Iran showed a decreasing trend due to the decrease in precipitation in recent years. A significant decreasing trend is computed at

the level of 0.05 for RX1day at 11.11%, RX3day at 10.34%, and RX5day at 10% of all stations.

Computed trends in climate zones are essential in several aspects. The increasing trend of extreme precipitation in the northern climate zones (Csa and Cfa), which have a humid climate, creates wetter conditions. This increase is consistent with the “wet gets wetter” theory by Tan et al. (2015). Since part of the precipitation on the Caspian Sea coast is related to convection, it is not unreasonable to expect that these changes are organized in connection with the spatial pattern of changes in the frequency of deep convection. On the southern coasts of Iran, an increasing trend was seen for the three Rx indices. Rahimzadeh et al. (2009) reported significant wet conditions in the coastal areas of the Caspian Sea and the Persian Gulf and dry conditions in the western regions of Iran between 1951 and 2003, which was also confirmed by Mahbod and Rafiee (2021) using a rain gauge data set.

Based on the Modified Mann–Kendall (Fig. 3) and Sen slope (Fig. 5) tests, we find that RX1day decreases at more than half of the stations during the period 1980 to 2019. Stations with higher positive trends are located in the north and west of Iran, while a significant part of eastern stations in Iran detected negative trends (Fig. 3). This trend coefficient is comparable to the research of Fathian et al. (2020) and Soltani et al. (2016) which also reported a similar trend for Iran’s extreme precipitation. The RX1day index has an increasing trend in four climate zones: Dsa, Csa, Cfa, and BSh. Also, at the station scale, at 44.89% of the stations, this extreme index has shown an increasing trend, which is 13.63% of all stations.

Westra et al., (2013) showed that 64% of Earth stations had an upward trend for the RX1day index. Comparing stations with an increasing trend in Iran with the global distribution increases the confidence that precipitation changes in Iran follow a general pattern on the Earth rather than being influenced by local factors. This result refers to the emergence of climatic signals in Iran. The trend of Rx indices is decreasing in parts of western and northwestern Iran (Lake Urmia basin). This decreasing trend was observed in the two mentioned regions with slight changes for all 12 extreme indices, indicating dry conditions in western and northwest Iran. Climate

Table 2

Mean, coefficient of variation (CV), trend using the nonparametric modified Mann–Kendall (MM–K) test, and trend magnitude based on Sen's slope estimator (SSE) for EPIs in different climate zones of Iran

Indices	Mean	CV %	Z	Q	Indices	Mean	CV %	Z	Q
BSh (arid, steppe, hot)									
CDD	121.26	15.03↓	−0.15	−0.64	R95pTOT	20.58	12.11↑	0.52	0.02
CWD	4.09	26.54↓	−1.12	−0.01	R99pTOT	5.61	39.66↑	0.07	0.35
PRCPTOT	376.12	31.80↓	−1.52	−2.71	RX1day	48.08	5.87↑	0.08	0.05
R10mm	11.98	−31.60↓	−1.25	−0.08	RX3day	69.82	52.05↓	−0.53	−0.19
R20mm	5.06	51.02↓	−0.76	−0.04	RX5day	77.71	50.83↓	−0.75	−0.30
R30mm	2.12	28.32↑	0.10	0.001	SDII	9.68	3.12↑	0.44	0.001
BSk (arid, steppe, cold)									
CDD	104.77	9.69↓	−0.36	−0.22	R95pTOT	19.11	10.24↑	0.14	0.02
CWD	4.17	9.47↓	−0.36	−0.004	R99pTOT	5.70	23.83↓	−0.01	−0.19
PRCPTOT	248.45	−20.13↓	−0.77	−0.90	RX1day	27.04	3.71↓	−0.34	−0.04
R10mm	7.40	1.44↓	−0.24	−0.02	RX3day	40.39	7.82↑	0.10	0.02
R20mm	1.65	1.65↓	−0.25	−0.006	RX5day	43.57	3.68↓	−0.02	−0.01
R30mm	0.42	6.97↓	−0.03	−0.002	SDII	5.91	25.81↑	0.68	0.01
BWh (arid, desert, hot)									
CDD	184.15	5.12↑	0.01	0.03	R95pTOT	17.58	38.13↓	−0.45	−0.06
CWD	2.78	23.67↓	−0.57	−0.01	R99pTOT	4.78	38.84↓	−0.01	−0.26
PRCPTOT	125.43	54.51↓	−1.28	−1.34	RX1day	29.96	36.08↓	−0.40	−0.09
R10mm	3.80	69.59↓	−1.05	−0.04	RX3day	39.44	17.77↓	−0.41	−0.15
R20mm	1.47	43.70↓	−0.62	−0.01	RX5day	43.03	19.42↓	−0.42	−0.17
R30mm	0.73	54.50↓	−0.39	−0.01	SDII	8.20	0.45↑	0.12	0.01
BWk (arid, desert, cold)									
CDD	124.41	1.25↑	0.14	0.13	R95pTOT	18.44	19.22↓	−0.31	−0.01
CWD	3.42	1.08↓	−0.12	−0.001	R99pTOT	5.23	55.54↑	0.008	−0.14
PRCPTOT	163.01	13.80↓	−0.98	−0.84	RX1day	22.23	16.74↓	−0.59	−0.07
R10mm	4.68	6.82↓	−0.61	−0.03	RX3day	29.80	28.73↓	−0.75	−0.13
R20mm	0.92	40.72↓	−0.47	−0.006	RX5day	33.24	17.80↓	−0.80	−0.15
R30mm	0.24	78.91↓	−0.13	−0.0004	SDII	5.49	5.53↑	0.27	0.004
Cfa (temperate, no dry season, hot summer)									
CDD	33.08	35.15↑	0.47	0.08	R95pTOT	23.97	34.13↑	0.44	0.02
CWD	8.61	28.48↑	1.44	0.04	R99pTOT	7.32	97.55↑	0.04	0.26
PRCPTOT	1728.03	17.84↑	0.36	1.96	RX1day	113.52	23.38↑	0.46	0.17
R10mm	48.66	16.42↓	−0.32	−0.04	RX3day	191.21	23.13↑	0.38	0.25
R20mm	28.66	18.27↑	0.75	0.10	RX5day	225.31	24.78↑	0.17	0.11
R30mm	17.72	26.25↑	0.86	0.10	SDII	16.32	12.76↑	2.13	0.05
Csa (temperate, dry summer, hot summer)									
CDD	77.33	12.41↑	0.40	0.04	R95pTOT	25.44	28.03↑	0.55	0.09
CWD	5.47	15.74↓	−0.49	−0.01	R99pTOT	8.05	43.59↑	0.12	0.12
PRCPTOT	859.74	4.88↓	−0.43	−0.15	RX1day	88.91	37.88↑	0.90	0.27
R10mm	25.21	7.16↓	−0.74	−0.03	RX3day	119.99	23.56↑	0.57	0.35
R20mm	12.15	2.88↓	−0.32	−0.02	RX5day	135.88	24.45↑	0.80	0.59
R30mm	6.66	10.91↑	0.67	0.03	SDII	11.43	17.65↑	1.38	0.04
Dsa (cold, dry summer, hot summer)									
CDD	102.24	2.91↓	−0.24	−0.25	R95pTOT	20.99	17.85↑	0.27	0.07
CWD	5.15	26.98↓	−1.05	−0.02	R99pTOT	6.50	19.97↓	−0.01	−0.24
PRCPTOT	560.53	25.55↓	−1.65	−2.89	RX1day	49.15	20.82↑	0.16	0.015
R10mm	18.32	9.79↓	−1.21	−0.10	RX3day	72.42	23.01↓	−0.42	−0.16
R20mm	7.20	4.75↓	−0.64	−0.03	RX5day	83.04	22.24↓	−0.79	−0.27
R30mm	3.40	12.37↑	0.08	0.003	SDII	8.70	8.19↑	0.39	0.01

Coefficient of variation (CV), Mann–Kendall trend test (Z), Theil–Sen slope estimator test (Q)

↑ upward variation; ↓ downward variation

Table 3

The change-point in precipitation extremes using Buishand's test

Station	<i>t</i>	Mu1	Mu2	Dif.
CWD				
Birjand	1998	4.389	2.833	-1.556
Chabahar	1998	3.063	1.833	-1.23
Saghez	1997	6.563	5.105	-1.458
Shiraz	1998	4.722	3.611	-1.111
R10mm				
Chabahar	1997	5.2	2.684	-2.516
Jask	1997	4.769	2.241	-2.528
Kermanshah	1994	16.143	12.364	-3.779
Khoramabad	1997	19.313	14.105	-5.208
Kish	1999	6.2	2.882	-3.318
Lengeh	1998	5.316	2.667	-2.649
Mashhad	1993	10.143	6.304	-3.839
Sanandaj	1997	17.647	11.789	-5.858
Saghez	1994	18.769	13.864	-4.905
Shahrud	1993	5.143	3.043	-2.1
Shiraz	2004	11.667	8.417	-3.25
R95pTOT				
Chabahar	2002	3.763	30.572	26.809
Gorgan	1994	18.091	27.723	9.632
RX1day				
Bushehr	2001	40.021	52.207	12.186
Chabahar	2006	30.442	60.672	30.23
RX5day				
Mashhad	1999	49.383	34.448	-14.93
Shahrud	1996	40.06	25.027	-15.03
PRCPTOT				
Bandarabbas	1998	210.782	116.265	-94.517
Birjand	1997	177.666	127.428	-50.238
Jask	1998	165.464	73.501	-91.963
Kerman	1997	148.731	108.993	-39.738
Kermanshah	1994	478.124	373.673	-104.451
Kish	1999	191.03	97.761	-93.269
Lengeh	1998	161.999	81.291	-80.708
Mashhad	1993	284.64	217.586	-67.054
Sanandaj	1997	486.435	338.462	-147.973
Saghez	1994	549.262	404.824	-144.438
Zabol	1999	66.301	37.343	-28.958
R20mm				
Kish	1999	3.05	1.294	-1.756
Lengeh	2000	2.429	0.875	-1.554
Sanandaj	1997	5.471	3.105	-2.366
Saghez	1994	6.154	3.773	-2.381
R99pTOT				
Bam	2010	1.115	18.534	17.419
Chabahar	2007	0	18.667	18.667
Khoramabad	2006	3.392	13.365	9.973
RX3day				
Nowshahr	1993	134.151	174.05	39.899
Shahrud	1996	36.012	23.654	-12.358
SDII				
Anzali	1996	15.331	17.119	1.788
Chabahar	2006	10.383	20.476	10.093

Table 3 *continued*

Station	<i>t</i>	Mu1	Mu2	Dif.
Sanandaj	1997	8.116	7.157	-0.959

Change-point year (*t*); pre-change-point mean (Mu1); post-change-point mean (Mu2); difference (Dif.)

change has played a significant role in the drying up of Lake Urmia, along with an anthropogenic factor. The trend of RX1day, RX3day, and RX5day is increasing in the northeast and east of Iran. The magnitude trend (Z-score of the MM-K test) of -2.52 was computed for the RX5day index in Mashhad and Zabol, which is significant at the level of 0.05.

The change-point of the Rx indices is presented in Table 3. The RX1day index in two coastal stations in southern Iran at Bushehr (difference before and after the change-point of 12.18 mm) and Chabahar (difference before and after the change-point of 30.23 mm) had a change-point in 2001 and 2006. The difference in precipitation before and after the change-point shows an increasing trend for this EPI in these two regions of Iran. In contrast, the RX5day index decreased, in which the two stations of Mashhad and Shahrud had a significant change-point at the level of 0.05 in 1999 and 1996. The difference before and after the change-point in Shahrud is -15.03 mm. The RX3day index also had a change-point for 1993 and 1996 at Nowshahr (Caspian Sea coast) and Shahrud stations. The index values in Shahrud are decreasing, and it is increasing for Nowshahr.

4.3. Heavy and Very Heavy Precipitation Days

The three indices of R10mm, R20mm, and R30mm for 1980–2019 were examined to investigate heavy and very heavy precipitation (Fig. 2). The hotspot of all three indices of heavy precipitation is on the Caspian Sea coast and then western Iran, which is located in the Csa, Cfa, and Dsa types of climate zone. The range of heavy and very heavy precipitation varies between 0.05 and 48.26 days across Iran.

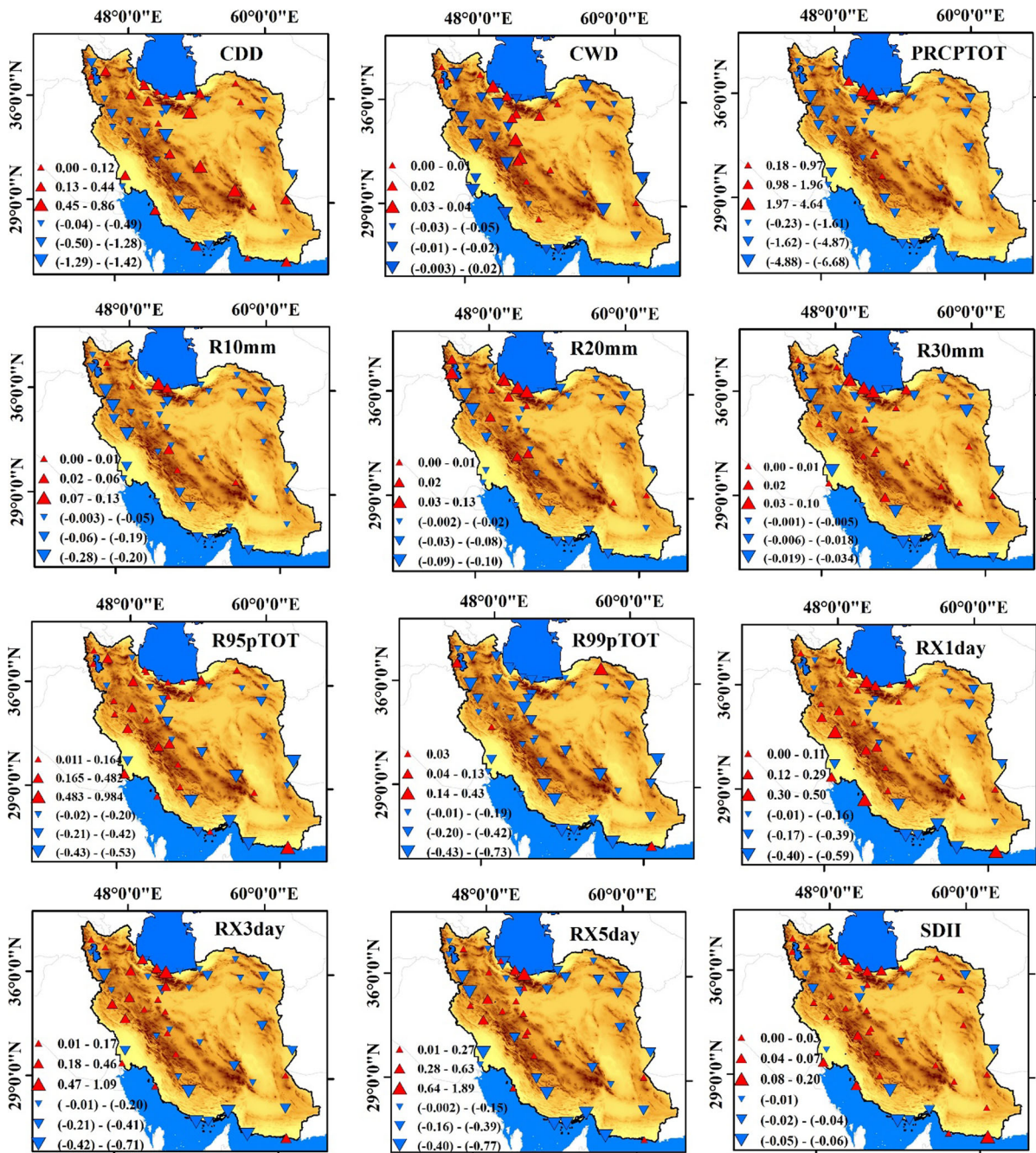


Figure 5

Annual magnitude of the trend of extreme precipitation indices over Iran in 1980–2019 (triangles = increasing trend, upside-down triangles = decreasing trend) (year^{-1})

The days with heavy and very heavy precipitation in the BSk, BWh, and BWk climate zones decreased in recent years. The highest decreasing trend of

R10mm is seen in the Dsa climate zone with -0.10 days/year (Fig. 4). Heavy precipitation days (R10mm) in 73.47% of all stations have a decreasing

trend, and this decreasing trend at 25% of them is significant at the 0.05 level (Fig. 3 and Table 2).

Also, the R10mm index has shown a decreasing trend in all climate zones. Very heavy precipitation indices of R20mm and R30mm have a decreasing trend at 63.27% (in 12.90% of the stations, the trend is significant at the level of 0.05) and 57.15% of the stations in Iran, respectively.

Of the three indices used to study the changes in heavy and very heavy precipitation in Iran, only two indices, R10mm (heavy precipitation) and R20mm (very heavy precipitation), had a change-point in the time series of the last four decades. In this regard, the number of stations with a change-point for the R10mm index is much higher, and 22.44% of stations show a significant change-point at the level of 0.05. The stations with change-points for heavy and very heavy precipitations are seen on the southern coasts (Chabahar, Bandar-e-Jask, Kish Island, Bandar Lengeh), west (Kermanshah, Khorramabad, Saqqez, and Sanandaj), northeast (Mashhad), the southern slopes of Alborz Mountains (Shahrud), and Shiraz station in the southwest of Iran (Table 3). Investigating the heavy precipitation change-point, it is found that most of the stations that show a change-point are located in western Iran. The difference between the average values of R10mm before and after the change-point in Khorramabad is -5.20 days, Sanandaj -5.85 days, and Saqqez -4.90 days. Similar to R10mm, the change-point of the very heavy

precipitation index (R20mm) is seen in the four stations of Kish Island, Bandar Lengeh, Saqqez, and Sanandaj, with the average R20mm changes of -2.36 and -2.38 days before and after the change-point, respectively.

4.4. Precipitation Intensity and Total Wet-Day Precipitation

The spatial distribution of the simple daily precipitation intensity index (SDII) shows that the precipitation intensity has increased uniformly in all climate zones of Iran in the last four decades (Table 2), as in many parts of the world (Kharin et al., 2018; Tabari, 2020).

Based on the results, the CV of SDII has increased in all climate zones of Iran. The CV for the climate zones of BSh, BSk, Bwh, Cfa, Csa, and Dsa has increased by 3.12, 25.81, 0.45, 53.5, 12.76, 17.65, and 8.19%, respectively. An increase in the intensity of precipitation and decrease in the annual precipitation can be seen in all climate zones of Iran (except Cfa, where annual precipitation has increased by 18.97%), especially in arid zones. The SDII showed an increasing trend in all climate zones of Iran from 1980 to 2019. However, only in the Cfa climate zone is the SDII index significant at the level of 0.05. The trend slope of the SDII in the mentioned zone is 0.05 mm/day/year (Fig. 5). SDII has a positive trend

Table 4

Correlation matrix between indices of precipitation extremes in Iran

Variables	CDD	CWD	PRCPTOT	R10mm	R20mm	R30mm	R95pTOT	R99pTOT	RX1day	RX3day	RX5day	SDII
CDD	1	-0.205	-0.170	-0.102	-0.127	-0.091	-0.220	-0.129	-0.232	-0.229	-0.234	-0.263
CWD	-0.205	1	0.664	0.627	0.562	0.451	0.457	0.370	0.564	0.603	0.650	0.229
PRCPTOT	-0.170	0.664	1	0.945	0.917	0.762	0.535	0.406	0.569	0.575	0.582	0.306
R10mm	-0.102	0.627	0.945	1	0.892	0.674	0.536	0.395	0.476	0.509	0.507	0.279
R20mm	-0.127	0.562	0.917	0.892	1	0.842	0.576	0.473	0.618	0.611	0.636	0.505
R30mm	-0.091	0.451	0.762	0.674	0.842	1	0.524	0.526	0.623	0.603	0.624	0.534
R95pTOT	-0.220	0.457	0.535	0.536	0.576	0.524	1	0.741	0.755	0.672	0.606	0.607
R99pTOT	-0.129	0.370	0.406	0.395	0.473	0.526	0.741	1	0.746	0.686	0.606	0.583
RX1day	-0.232	0.564	0.569	0.476	0.618	0.623	0.755	0.746	1	0.896	0.855	0.606
RX3day	-0.229	0.603	0.575	0.509	0.611	0.603	0.672	0.686	0.896	1	0.959	0.660
RX5day	-0.234	0.650	0.582	0.507	0.636	0.624	0.606	0.606	0.855	0.959	1	0.661
SDII	-0.263	0.229	0.306	0.279	0.505	0.534	0.607	0.583	0.606	0.660	0.661	1

Values in bold are different from 0 with a significance level $\alpha = 0.05$

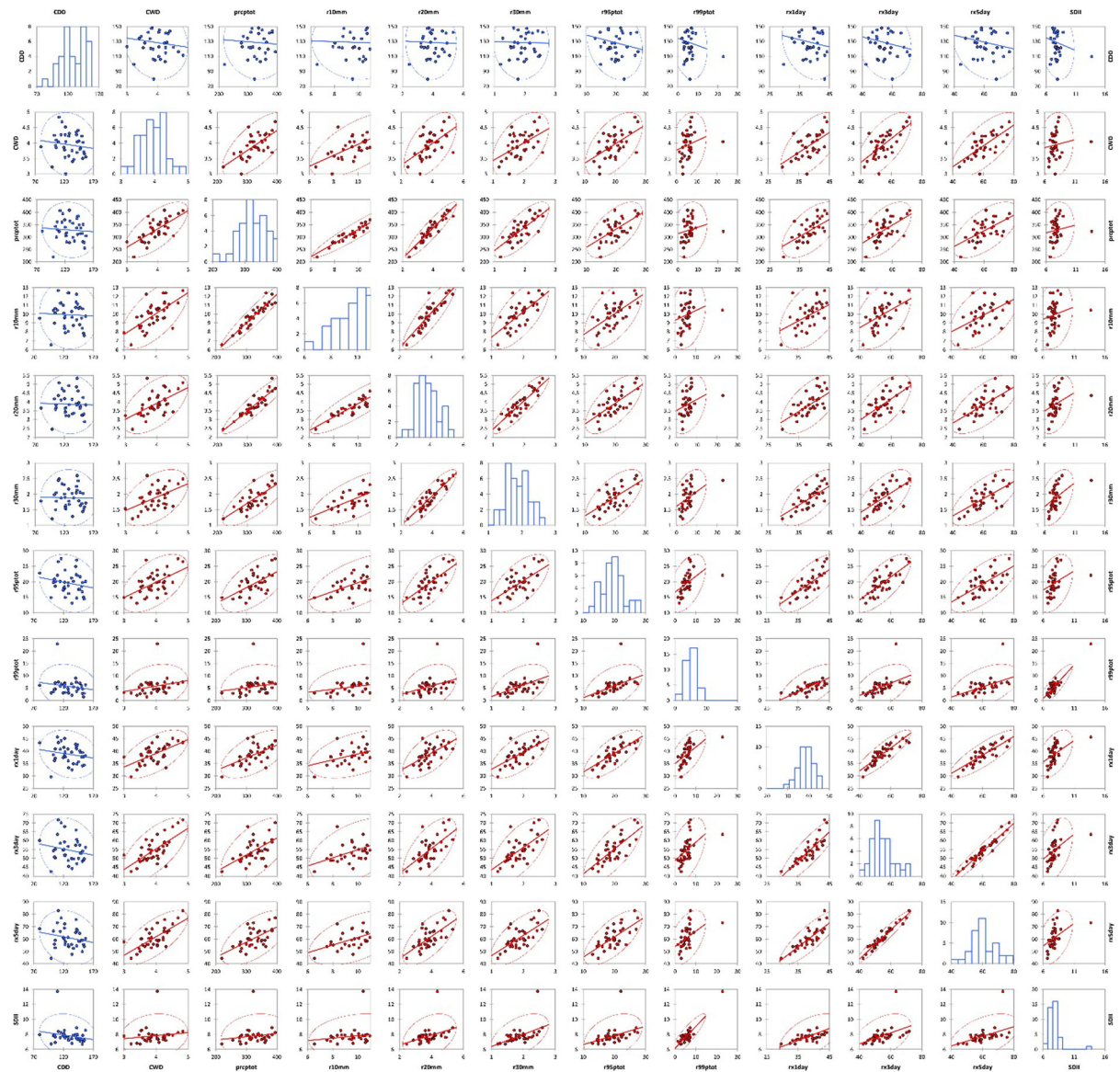


Figure 6

Scatter plot correlation matrix EPIs in Iran. Each row and column represent an extreme precipitation index, and diameter histograms represent changes in that index throughout the year

in 71.42% of stations, of which 22.58% of them are significant ($\alpha = 0.05$).

The SDII change-point is significant in Bandar Anzali, Chabahar, and Sanandaj. These three stations are located in the southern Caspian Sea coast, the coast of the Oman Sea, and western Iran. Having the change-point of SDII in these three regions is very important, especially for the Chabahar station. This

station is located in the semiarid region of Iran, and its total annual precipitation is about 120 mm; precipitation at this station has increased by 10 mm compared to before the change-point in 2006. This increase plays a vital role in flooding and soil erosion in this region. Precipitation in this region is affected by the Asian summer monsoon (ASM), so it seems that the ASM has strengthened in recent years, which

could be due to changes in the large-scale atmospheric circulation under global warming. The trend of PRCPTOT is decreasing in all climate zones except for Cfa, which is increasing. The maximum changes in PRCPTOT in Iran were related to Dsa and BSh climate zones at 2.89 and 2.71 mm/year, respectively. However, the trend slope (Fig. 5) is not significant ($\alpha = 0.05$).

4.5. Consecutive Wet Days (CWD) and Consecutive Dry Days (CDD)

The CWD index ranges from 2.24 days in southeastern Iran to 8.55 days on the southern Caspian Sea coast of Iran (Fig. 2). The CWD has a decreasing trend with a steep slope from northwest to southeast Iran. The hotspot of CWD in Iran is in the climate zones of Cfa, Csa, and Dsa. The CWD has a decreasing trend in all climate zones, except the Cfa which showed an increasing trend with 0.04 days/year (Fig. 5).

The CWD at 73.47% of the studied stations showed a decreasing trend, of which 13.88% were significant ($\alpha = 0.05$).

The study of CWD for Birjand, Chabahar, Saqqez, and Shiraz has shown a significant change-point; the average CWD after the change-point was less than before the change-point. The CWD has decreased by 1 day during the last four decades (Table 3). The contribution of the CWD index in Iran is between 0.61 and 2.34% of the total days of the year. For example, 2.34% of the total days of the year in Bandar Anzali on the southwest coast of the Caspian Sea are consecutively wet days.

CDD is precisely the opposite of CWD, so the minimum average of the country with 30.14 days/year has been seen on the southwest coast of the Caspian Sea, and the maximum index of 213.70 days/year is detected in southeastern Iran.

Above 36° north, CDD is less than 50 days/year, and below 36° N in all regions of Iran, CDD is more than 100 days/year. Similarly, the contribution of CDD above 36° N is less than 10%, and below this latitude, it reaches a maximum of 58.54%. A critical and worrying point is the increase of consecutive dry days in wet areas of Iran such as Cfa and Csa so that consecutive dry days in the Cfa zone (Anzali in the

southwest of the Caspian Sea) have increased by 35% over the last four decades. In the whole country, consecutive dry days in 46.93% of Iran have shown an increasing trend. A decreasing CDD and simultaneously increasing CWD in BWh, BWk, and Csa climate zones means increasing the amount of heavy precipitation in these climate zones of Iran. Also, at 10.26% of the stations, CDD is decreasing, and CWD is increasing simultaneously.

4.6. Cross-Correlation Extreme Precipitation Indices (EPIs) in Iran

To better present the relationship between extreme precipitation indices in Iran, a cross-correlation and scatter plot correlation matrix was prepared using the Spearman rank correlation method and is presented in Table 4 and Fig. 6. The correlation between extreme precipitation indices (EPIs) in Iran is between -0.263 and 0.959 . A strong negative correlation is between CDD and SDII, which is not significant ($\alpha = 0.05$). In contrast, the strong positive correlation, which is significant at the level of 0.05, is between the two indices of RX5day and RX3day. PRCPTOT, RX1day, RX3day, and RX5day indices showed a strong correlation with EPIs. PRCPTOT has a significant and robust correlation with all EPIs at 95%, except for CDD and SDII in Iran. Thus, EPIs may reflect PRCPTOT changes in Iran to some extent. Ajjur and Riffi (2020) achieved a similar result in the Gaza Strip for EPIs. The Spearman rank correlation coefficient for RX1day, RX3day, and RX5day indices with PRCPTOT index was computed as 0.56, 0.57, and 0.58, respectively. However, some indices are different in terms of correlation relationships.

The CDD index has negatively correlated to all EPIs in Iran. However, this correlation is not significant for any of them. Spatial analysis of CDD and SDII correlation has shown that in transitional areas from a humid climate zone to a dry one, this relationship is more robust (for example, stations located on both sides of the Zagros or north and south Alborz). Also, there is a strong and positive correlation between precipitation intensity indices (RX1day, RX3day, and RX5day) with heavy precipitation indices (R10mm, R20mm, and R30mm); the

Spearman rank correlation test coefficients between RX1day and R30mm in Iran show 0.62, which is significant at the 95% confidence level. Specifically, among 21 stations, R10mm has also increased by 38.09% with the increase of the RX1day index.

With an increase of precipitation days by more than one mm, the frequency of heavy precipitation increases in Iran. The R10mm index has no significant correlation with precipitation intensity. In contrast, the RX5day index has a crucial role in precipitation intensity (SDII) in Iran; the correlation value is 0.661, significant at the 95% confidence interval. The consecutive wet day index (CWD) shows a significant positive correlation with all EPIs, except for CDD and SDII. The strong correlation between R95pTOT and SDII (0.607) indicates that indices based on precipitation percentile are subject to change with precipitation intensity in Iran. In general, duration-based EPIs had a weak correlation with frequency indices and a strong correlation with intensity indices.

5. Conclusion

Compared to many studies that applied only 95th and 99th percentiles of precipitation (Alavinia and Zarei, 2021; Fathian et al., 2020; Ghiami-Shamami et al., 2019; Rahimzadeh et al., 2009; Rahimi & Fatemi, 2019; Soltani et al., 2016), new indices such as R30mm and RX3day and new combined index ($100 * r_{95p}$ or $r_{99p} / \text{PRCPTOT}$) were used for detecting extreme precipitation in Iran. The 95th (99th) percentile is not a good index of precipitation intensity because the 95th (99th) index computes the percentage of daily precipitation events, whereas R95pTOT (99th) computes the total precipitation amount on rainy days when $\text{RR} \geq 95\text{th}$ (99th).

The results showed that the areas with high CWD are mainly located in the Caspian Sea coast and northwest and western regions of Iran, while the areas with CDD are mainly located in the central and eastern parts of Iran. The hotspot of heavy and very heavy precipitation indices and precipitation on days 1, 3, and 5 in Iran is located in the Cfa, Csa, and Dsa climate zones.

The consecutive wet day index (CWD), total precipitation on wet days (PRCPTOT), and heavy precipitation (R10mm) showed a decreasing trend of 73.47, 87.46, and 73.47% the in the last four decades, respectively.

The precipitation intensity index (SDII) and percentile-based indices (R95pTOT and R99pTOT) showed an increasing trend at 71.42, 51.02, and 57.14% of the total stations, respectively, during the last four decades. Globally, the increasing trend in precipitation event frequency under global warming (Benestad, 2018; Norris et al., 2019) has been confirmed.

The consecutive wet days (CWD), total annual precipitation on wet days (PRCPTOT), heavy precipitation (R10mm), and very heavy precipitation (R20mm) had a decreasing trend and change-point in western Iran.

The west of Iran is a mountainous region where most of the winter precipitation is supplied by the Mediterranean Sea system (Alijani and Harman, 1985; Ghalhari et al., 2016). Therefore, the decrease in annual precipitation in western Iran may be due to the poleward movement of the northern hemisphere storms under climate change conditions, which weakens the Mediterranean storm track and reduces the number of cyclones crossing the Mediterranean (Nissen et al., 2014). In this regard, Flocas et al. (2010) showed that the central frequency of Mediterranean cyclones is in January, and they decrease by August from the western Mediterranean to the east.

Also, precipitation in Iran is affected by other factors such as the El Niño-Southern Oscillation (ENSO) (Nazemosadat & Ghasemi, 2004), Southern Oscillation Index (SOI) (Roushangar et al., 2018), North Atlantic Oscillation (NAO) (Masih et al., 2011), Arabian anticyclone (Raziei et al., 2012), Red Sea Trough (Mofidi, 2005), and Asian summer monsoon (Babaeian & Rezazadeh, 2018). Changes in the Asian summer monsoon, to some extent, can determine the amount of precipitation in southeastern Iran.

Alizadeh and Choobari et al. (2016) showed that in the Lake Urmia basin, arable land has increased significantly in recent decades. Urmia is located in northwestern Iran. During the last four decades,

CDD, CWD, R20mm, R30mm, R95pTOT, R99pTOT, and SDII indices showed an increasing trend. Daniels et al. (2015) also pointed out that urban land-use change is a factor in precipitation increase in the Lake Urmia basin. However, the spatial pattern of precipitation changes in Iran is complex and has different regional trends. Changes in Iran's precipitation result from the increasing intensity and are more important for changes in the average precipitation. A significant contribution to Iran's annual precipitation occurs in a few days of the year in the form of heavy and very heavy precipitation. In other words, the contribution of extreme indices in the annual precipitation in Iran has increased over the past four decades.

Acknowledgements

Abbasali Dadashi-Roudbari was supported by a grant from Ferdowsi University of Mashhad (no. FUM 14002794075). We would like to thank the Iran Meteorological Organization (IRIMO) for providing the necessary data and information.

Author Contributions Conceived and designed the analysis: Azar Zarrin and Abbasali Dadashi-Roudbari. Collected the data: Azar Zarrin and Abbasali Dadashi-Roudbari. Contributed data or analysis tools: Azar Zarrin and Abbasali Dadashi-Roudbari. Performed the analysis: Azar Zarrin and Abbasali Dadashi-Roudbari. Wrote the paper: Azar Zarrin and Abbasali Dadashi-Roudbari. Writing—review and editing: Azar Zarrin and Abbasali Dadashi-Roudbari.

Funding

Vice Chancellor for Research of Ferdowsi University of Mashhad.

Availability of Data and Material

Not applicable.

Code Availability

The R package used in this paper is available on github (<https://github.com/ECCC-CDAS/RCLimDex>).

Declarations

Conflict of Interest The authors declare that they have no conflict of interest.

Ethics Approval We approve the ethical responsibilities of authors.

Consent to Participate Not applicable.

Consent for Publication Not applicable.

Publisher's Note Springer Nature remains neutral with regard to jurisdictional claims in published maps and institutional affiliations.

REFERENCES

- Ajjur, S. B., & Riffi, M. I. (2020). Analysis of the observed trends in daily extreme Precipitation indices in Gaza Strip during 1974–2016. *International Journal of Climatology*. <https://doi.org/10.1002/joc.6576>
- Alavinia, S. H., & Zarei, M. (2021). Analysis of spatial changes of extreme precipitation and temperature in Iran over a 50-year period. *International Journal of Climatology*, 41, E2269–E2289.
- Alexander, L. V., Fowler, H. J., Bador, M., Behrangi, A., Donat, M. G., Dunn, R., & Venugopal, V. (2019). On the use of indices to study extreme precipitation on sub-daily and daily timescales. *Environmental Research Letters*, 14(12), 125008.
- Alijani, B., & Harman, J. R. (1985). Synoptic climatology of precipitation in Iran. *Annals of the Association of American Geographers*, 75(3), 404–416.
- Alijani, B., O'Brien, J., & Yarnal, B. (2008). Spatial analysis of precipitation intensity and concentration in Iran. *Theoretical and Applied Climatology*, 94(1), 107–124.
- Alizadeh-Choobari, O., Ahmadi-Givi, F., Mirzaei, N., & Oulad, E. (2016). Climate change and anthropogenic impacts on the rapid shrinkage of Lake Urmia. *International Journal of Climatology*, 36(13), 4276–4286.
- Babaeian, I., & Rezazadeh, P. (2018). On the relationship between Indian monsoon withdrawal and Iran's fall precipitation onset. *Theoretical and Applied Climatology*, 134(1–2), 95–105.
- Beck, H. E., Zimmermann, N. E., McVicar, T. R., Vergopolan, N., Berg, A., & Wood, E. F. (2018). Present and future Köppen-Geiger climate classification maps at 1-km resolution. *Scientific Data*, 5(1), 1–12.
- Benestad, R. E. (2018). Implications of a decrease in the precipitation area for the past and the future. *Environmental Research Letters*, 13(4), 044022.
- Beniston, M. (2015). Ratios of record high to record low temperatures in Europe exhibit sharp increases since 2000 despite a slowdown in the rise of mean temperatures. *Climatic Change*, 129(1–2), 225–237.
- Buishand, T. A. (1982). Some methods for testing the homogeneity of rainfall records. *Journal of Hydrology*, 58(1–2), 11–27.
- Cardoso Pereira, S., Marta-Almeida, M., Carvalho, A. C., & Rocha, A. (2020). Extreme precipitation events under climate change in

- the Iberian Peninsula. *International Journal of Climatology*, 40(2), 1255–1278.
- Carpenter, S. R., Booth, E. G., & Kucharik, C. J. (2018). Extreme precipitation and phosphorus loads from two agricultural watersheds. *Limnology and Oceanography*, 63(3), 1221–1233.
- Chapagain, D., Dhaubanjari, S., & Bharati, L. (2021). Unpacking future climate extremes and their sectoral implications in western Nepal. *Climatic Change*, 168(1), 1–23.
- Dadashi-Roudbari, A., & Ahmadi, M. (2020). Evaluating temporal and spatial variability and trend of aerosol optical depth (550 nm) over Iran using data from MODIS on board the Terra and Aqua satellites. *Arabian Journal of Geosciences*, 13(6), 1–23.
- Dadashi-Roudbari, A., & Ahmadi, M. (2021). An assessment of change point and trend of diurnal variation of dust storms in Iran: A multi-instrumental approach from in situ, multi-satellite, and reanalysis dust product. *Meteorology and Atmospheric Physics*, 133(5), 1523–1544.
- Daniels, E. E., Hutjes, R. W., Lenderink, G., Ronda, R. J., & Holtlag, A. A. (2015). Land surface feedbacks on spring precipitation in the Netherlands. *Journal of Hydrometeorology*, 16(1), 232–243.
- Darand, M., Dostkamyan, M., & Rehmani, M. I. A. (2017). Spatial autocorrelation analysis of extreme precipitation in Iran. *Russian Meteorology and Hydrology*, 42(6), 415–424.
- de Vries, A. J., Tyrllis, E., Edry, D., Krichak, S. O., Steil, B., & Lelieveld, J. (2013). Extreme precipitation events in the Middle East: Dynamics of the Active Red Sea Trough. *Journal of Geophysical Research: Atmospheres*, 118(13), 7087–7108.
- Donat, M. G., Alexander, L. V., Yang, H., Durre, I., Vose, R., Dunn, R. J. H., & Kitching, S. (2013). Updated analyses of temperature and precipitation extreme indices since the beginning of the twentieth century: The HadEX2 dataset. *Journal of Geophysical Research: Atmospheres*, 118(5), 2098–2118.
- Donat, M. G., Lowry, A. L., Alexander, L. V., O’Gorman, P. A., & Maher, N. (2017). Addendum: More extreme precipitation in the world’s dry and wet regions. *Nature Climate Change*, 7(2), 154–158.
- Donat, M. G., Angéilil, O., & Ukkola, A. M. (2019). Intensification of precipitation extremes in the world’s humid and water-limited regions. *Environmental Research Letters*, 14(6), 065003.
- Dravitzki, S., & McGregor, J. (2011). Extreme precipitation of the Waikato region. *New Zealand. International Journal of Climatology*, 31(12), 1803–1812.
- Fathian, F., Ghadami, M., Haghghi, P., Amini, M., Naderi, S., & Ghaedi, Z. (2020). Assessment of changes in climate extremes of temperature and precipitation over Iran. *Theoretical and Applied Climatology*, 141, 1119–1133. <https://doi.org/10.1007/s00704-020-03269-2>
- Flocas, H. A., Simmonds, I., Kouroutzoglou, J., Keay, K., Hatzaki, M., Bricolas, V., & Asimakopoulos, D. (2010). On cyclonic tracks over the eastern Mediterranean. *Journal of Climate*, 23(19), 5243–5257.
- Ghalhari, G. F., Roudbari, A. D., & Asadi, M. (2016). Identifying the spatial and temporal distribution characteristics of precipitation in Iran. *Arabian Journal of Geosciences*, 9(12), 1–12.
- Ghiami-Shamami, F., Sabziparvar, A. A., & Shinoda, S. (2019). Long-term comparison of the climate extremes variability in different climate types located in coastal and inland regions of Iran. *Theoretical and Applied Climatology*, 136(3–4), 875–897.
- Guo, X., Wu, Z., He, H., Du, H., Wang, L., Yang, Y., & Zhao, W. (2018). Variations in the start, end, and length of extreme precipitation period across China. *International Journal of Climatology*, 38(5), 2423–2434.
- Hamed, K. H. (2008). Trend detection in hydrologic data: The Mann-Kendall trend test under the scaling hypothesis. *Journal of Hydrology*, 349(3–4), 350–363.
- Hay, J. E., Easterling, D., Ebi, K. L., Kitoh, A., & Parry, M. (2016). Conclusion to the special issue: Observed and projected changes in weather and climate extremes. *Weather and Climate Extremes*, 11, 103–105.
- Heureux, A. M. C., Alvar-Beltrán, J., Manzanar, R., Ali, M., Wahaj, R., Dowlatchahi, M., Afzaal, M., Kazmi, D., Ahmed, B., Salehnia, N., & Fujisawa, M. (2022). Climate Trends and Extremes in the Indus River Basin, Pakistan: Implications for Agricultural Production. *Atmosphere*, 13(3), 378.
- Hoegh-Guldberg, O., Jacob, D., Bindi, M., Brown, S., Camilloni, I., Diedhiou, A., & Hijioka, Y. (2018). Impacts of 1.5 C global warming on natural and human systems. Global warming of 1.5° C. An IPCC Special Report.
- Intergovernmental Panel on Climate Change (IPCC), (2013). In: Stocker, T.F., et al. (Eds.), *Climate Change 2013: The Physical Science Basis: Working Group I Contribution to the Fifth Assessment Report of the Intergovernmental Panel on Climate Change*. Cambridge Univ Press, Cambridge, United Kingdom and New York, NY, USA
- IPCC (2012). *Managing the Risks of Extreme Events and Disasters to Advance Climate Change Adaptation. A Special Report of Working Groups I and II of the Intergovernmental Panel on Climate Change*. Cambridge University Press, Cambridge, UK, and New York, NY, USA, 582 pp
- Javanmard, S., Yatagai, A., Nodzu, M. I., BodaghJamali, J., & Kawamoto, H. (2010). Comparing high-resolution gridded precipitation data with satellite rainfall estimates of TRMM_3B42 over Iran. *Advances in Geosciences*, 25, 119–125.
- Kendall, M. G. (1948). Rank correlation methods.
- Khalilii, K., Tahoudi, M. N., Mirabbasi, R., & Ahmadi, F. (2016). Investigation of spatial and temporal variability of precipitation in Iran over the last half century. *Stochastic Environmental Research and Risk Assessment*, 30(4), 1205–1221.
- Kharin, V. V., Zwiers, F. W., Zhang, X., & Wehner, M. (2013). Changes in temperature and precipitation extremes in the CMIP5 ensemble. *Climatic Change*, 119(2), 345–357.
- Kharin, V. V., Flato, G. M., Zhang, X., Gillett, N. P., Zwiers, F., & Anderson, K. J. (2018). Risks from climate extremes change differently from 1.5 C to 2.0 C depending on rarity. *Earth’s Future*, 6(5), 704–715.
- Kiany, M. S. K., Masoodian, S. A., Balling, R. C., Jr., & Montazeri, M. (2020). Evaluation of the TRMM 3B42 product for extreme precipitation analysis over southwestern Iran. *Advances in Space Research*, 66(9), 2094–2112.
- Kirschbaum, D., Kapnick, S. B., Stanley, T., & Pascale, S. (2020). Changes in extreme precipitation and landslides over High Mountain Asia. *Geophysical Research Letters*, 47(4), e2019GL085347.
- Kunkel, K. E. (2003). North American trends in extreme precipitation. *Natural Hazards*, 29(2), 291–305.
- Leander, R., Buishand, T. A., & Tank, A. K. (2014). An alternative index for the contribution of precipitation on very wet days to the total precipitation. *Journal of Climate*, 27(4), 1365–1378.
- Li, Y. G., He, D., Hu, J. M., & Cao, J. (2015). Variability of extreme precipitation over Yunnan Province, China 1960–2012. *International Journal of Climatology*, 35(2), 245–258.

- Liu, H., Remer, L. A., Huang, J., Huang, H. C., Kondragunta, S., Laszlo, I., & Jackson, J. M. (2014). Preliminary evaluation of S-NPP VIIRS aerosol optical thickness. *Journal of Geophysical Research: Atmospheres*, 119(7), 3942–3962.
- Maghrabi, A. H., & Alotaibi, R. N. (2018). Long-term variations of AOD from an AERONET station in the central Arabian Peninsula. *Theoretical and Applied Climatology*, 134(3–4), 1015–1026.
- Mahbod, M., & Rafiee, M. R. (2021). Trend analysis of extreme precipitation events across Iran using percentile indices. *International Journal of Climatology*, 41(2), 952–969.
- Mann, H. B. (1945). Nonparametric tests against trend. *Econometrica. Journal of the Econometric Society*, 13, 245–259.
- Masih, I., Uhlenbrook, S., Maskey, S., & Smakhtin, V. (2011). Streamflow trends and climate linkages in the Zagros Mountains, Iran. *Climatic Change*, 104(2), 317–338.
- Masson-Delmotte, V., Zhai, P., Pörtner, H. O., Roberts, D., Skea, J., Shukla, P. R., & Waterfield, T. (2018). Global warming of 1.5 C. *An IPCC Special Report on the Impacts of Global Warming of 1.5 C*.
- Mofidi, A. (2005). Synoptic Climatology of Heavy Rainfalls with Origin of Red Sea Region in the Middle East. *GEOGRAPHICAL RESEARCH*, 19(4), 71–93. (In Persian).
- Myers, L., & Sirois, M. J. (2004). Spearman Correlation Coefficients, Differences between. *Encyclopedia of statistical sciences*.
- Najafi, M. R., & Moazami, S. (2016). Trends in total precipitation and magnitude–frequency of extreme precipitation in Iran, 1969–2009. *International Journal of Climatology*, 36(4), 1863–1872.
- Nazemosadat, M. J., & Ghasemi, A. R. (2004). Quantifying the ENSO-related shifts in the intensity and probability of drought and wet periods in Iran. *Journal of Climate*, 17(20), 4005–4018.
- Nissen, K. M., Leckebusch, G. C., Pinto, J. G., & Ulbrich, U. (2014). Mediterranean cyclones and windstorms in a changing climate. *Regional Environmental Change*, 14(5), 1873–1890.
- Norris, J., Chen, G., & Neelin, J. D. (2019). Changes in frequency of large precipitation accumulations over land in a warming climate from the CESM Large Ensemble: The roles of moisture, circulation, and duration. *Journal of Climate*, 32(17), 5397–5416.
- Palharini, R. S. A., Vila, D. A., Rodrigues, D. T., Quispe, D. P., Palharini, R. C., de Siqueira, R. A., & de Sousa Afonso, J. M. (2020). Assessment of the extreme precipitation by satellite estimates over South America. *Remote Sensing*, 12(13), 2085.
- Pour, S. H., Wahab, A. K. A., & Shahid, S. (2020). Spatiotemporal changes in precipitation indicators related to bioclimate in Iran. *Theoretical and Applied Climatology*, 141(1), 99–115.
- Prein, A. F., Rasmussen, R. M., Ikeda, K., Liu, C., Clark, M. P., & Holland, G. J. (2017). The future intensification of hourly precipitation extremes. *Nature Climate Change*, 7(1), 48–52.
- Rahimi, M., & Fatemi, S. S. (2019). Mean versus extreme precipitation trends in Iran over the period 1960–2017. *Pure and Applied Geophysics*, 176(8), 3717–3735.
- Rahimzadeh, F., Asgari, A., & Fattahi, E. (2009). Variability of extreme temperature and precipitation in Iran during recent decades. *International Journal of Climatology: A Journal of the Royal Meteorological Society*, 29(3), 329–343.
- Rahman, M. S., & Islam, A. R. M. T. (2019). Are precipitation concentration and intensity changing in Bangladesh overtimes? Analysis of the possible causes of changes in precipitation systems. *Science of the Total Environment*, 690, 370–387.
- Raziei, T., Mofidi, A., Santos, J. A., & Bordi, I. (2012). Spatial patterns and regimes of daily precipitation in Iran in relation to large-scale atmospheric circulation. *International Journal of Climatology*, 32(8), 1226–1237.
- Roushangar, K., Alizadeh, F., & Adamowski, J. (2018). Exploring the effects of climatic variables on monthly precipitation variation using a continuous wavelet-based multiscale entropy approach. *Environmental Research*, 165, 176–192.
- Rousta, I., Karampour, M., Doostkamian, M., Olafsson, H., Zhang, H., Mushore, T. D., & Vargas, E. R. M. (2020). Synoptic-dynamic analysis of extreme precipitation in Karoun River Basin, Iran. *Arabian Journal of Geosciences*, 13(2), 1–16.
- Salehi, S., Dehghani, M., Mortazavi, S. M., & Singh, V. P. (2020). Trend analysis and change point detection of seasonal and annual precipitation in Iran. *International Journal of Climatology*, 40(1), 308–323.
- Schär, C., Ban, N., Fischer, E. M., Rajczak, J., Schmidli, J., Frei, C., & O’Gorman, P. A. (2016). Percentile indices for assessing changes in heavy precipitation events. *Climatic Change*, 137(1–2), 201–216.
- Sen, P. K. (1968). Estimates of the regression coefficient based on Kendall’s tau. *Journal of American Statistical Association*, 63, 1379–1389.
- Shaffie, S., Mozaffari, G., & Khosravi, Y. (2019). Determination of extreme precipitation threshold and analysis of its effective patterns (case study: West of Iran). *Natural Hazards*, 99(2), 857–878.
- Shongwe, M. E., van Oldenborgh, G. J., Van den Hurk, B., & van Aalst, M. (2011). Projected changes in mean and extreme precipitation in Africa under global warming. Part II: East Africa. *Journal of climate*, 24(14), 3718–3733.
- Soltani, M., Laux, P., Kunstmann, H., Stan, K., Sohrabi, M. M., Molanejad, M., & Martin, M. V. (2016). Assessment of climate variations in temperature and precipitation extreme events over Iran. *Theoretical and Applied Climatology*, 126(3), 775–795.
- Some’e, B. S., Ezani, A., & Tabari, H. (2012). Spatiotemporal trends and change point of precipitation in Iran. *Atmospheric Research*, 113, 1–12.
- Stocker, T. F., Qin, D., Plattner, G. K., Tignor, M., Allen, S. K., Boschung, J., & Midgley, P. M. (2013). Climate change 2013: The physical science basis. Contribution of working group I to the fifth assessment report of the intergovernmental panel on climate change, 1535.
- Tabari, H. (2020). Climate change impact on flood and extreme precipitation increases with water availability. *Scientific Reports*, 10(1), 1–10.
- Tabari, H., & Willems, P. (2018). Seasonally varying footprint of climate change on precipitation in the Middle East. *Scientific Reports*, 8(1), 1–10.
- Tabari, H., AghaKouchak, A., & Willems, P. (2014). A perturbation approach for assessing trends in precipitation extremes across Iran. *Journal of Hydrology*, 519, 1420–1427.
- Talchabhadel, R., Karki, R., Thapa, B. R., Maharjan, M., & Parajuli, B. (2018). Spatio-temporal variability of extreme precipitation in Nepal. *International Journal of Climatology*, 38(11), 4296–4313.
- Tan, J., Jakob, C., Rossow, W. B., & Tselioudis, G. (2015). Increases in tropical rainfall driven by changes in frequency of organized deep convection. *Nature*, 519(7544), 451–454.

- Tebaldi, C., & Wehner, M. F. (2018). Benefits of mitigation for future heat extremes under RCP4.5 compared to RCP8.5. *Climatic Change*, *146*(3–4), 349–361.
- Thiel, H. (1950). A rank-invariant method of linear and polynomial regression analysis, Part 3. In Proceedings of Koninklijke Nederlandse Akademie van Wetenschappen A (Vol. 53, pp. 1397–1412).
- Trenberth, K. E., Dai, A., Rasmussen, R. M., & Parsons, D. B. (2003). The changing character of precipitation. *Bull Am Meteorol Soc*, *84*(9), 1205–1218.
- UNISDR (2015). The Human Cost of Weather-Related Disasters 1995–2015. United Nations Initiative for Disaster Reduction. Available at: https://www.unisdr.org/files/48588_unisdrannualreport2015evs.pdf.
- Wasko, C., Lu, W. T., & Mehrotra, R. (2018). Relationship of extreme precipitation, dry-bulb temperature, and dew point temperature across Australia. *Environmental Research Letters*, *13*(7), 074031.
- Westra, S., Alexander, L. V., & Zwiers, F. W. (2013). Global increasing trends in annual maximum daily precipitation. *Journal of Climate*, *26*(11), 3904–3918.
- Yue, S., & Hashino, M. (2003). Temperature trends in Japan: 1900–1996. *Theoretical and Applied Climatology*, *75*(1–2), 15–27.
- Zarrin, A., & Dadashi-Roudbari, A. (2021). Projection of future extreme precipitation in Iran based on CMIP6 multi-model ensemble. *Theoretical and Applied Climatology*, *144*(1), 643–660.
- Zhang, X., Alexander, L., Hegerl, G. C., Jones, P., Tank, A. K., Peterson, T. C., & Zwiers, F. W. (2011). Indices for monitoring changes in extremes based on daily temperature and precipitation data. *Wiley Interdisciplinary Reviews: Climate Change*, *2*(6), 851–870.
- Zhang, W., Zhou, T., Zou, L., Zhang, L., & Chen, X. (2018). Reduced exposure to extreme precipitation from 0.5 C less warming in global land monsoon regions. *Nature Communications*, *9*(1), 1–8.
- Zhang, X., Aguilar, E., Sensoy, S., Melkonyan, H., Tagiyeva, U., Ahmed, N., & Wallis, T. (2005). Trends in Middle East climate extreme indices from 1950 to 2003. *Journal of Geophysical Research: Atmospheres*, *110*(D22).
- Zolina, O., Simmer, C., Kapala, A., & Gulev, S. (2005). On the robustness of the estimates of centennial-scale variability in heavy precipitation from station data over Europe. *Geophysical Research Letters*. <https://doi.org/10.1029/2005GL023231>

(Received February 6, 2022, revised May 20, 2022, accepted June 22, 2022, Published online July 12, 2022)